Human Molecular Genetics, 2023, Vol. 32, 7, 1102–1113
https://doi.org/10.1093/hmg/ddac268
Advance access publication date 29 October 2022
Original Article

TFIIH mutations can impact on translational fidelity of the ribosome

Fatima Khalid[1], Tamara Phan[1], Mingyue Qiang[1], Pallab Maity[1], Theresa Lasser[1], Sebastian Wiese[2], Marianna Penzo[3], Marius Alupei[1], Donata Orioli[4], Karin Scharffetter-Kochanek[1] and Sebastian Iben[1,*]

[1]Department of Dermatology and Allergic Diseases, Ulm University Medical Center, 89081 Ulm, Germany
[2]Core Unit of Mass Spectrometry and Proteomics, Ulm University Medical Center, 89081 Ulm, Germany
[3]Department of Experimental, Diagnostic and Specialty Medicine, University of Bologna, 40138 Bologna, Italy
[4]Institute of Molecular Genetics, Consiglio Nazionale delle Ricerche, 27100 Pavia, Italy
*To whom correspondence should be addressed at: Department of Dermatology and Allergic Diseases, Ulm University Medical Center, Albert-Einstein Allee 23, 89081 Ulm, Germany. Tel: +49 73150057645; Fax: +49 73150057660; Email: sebastian.iben@uni-ulm.de

Abstract

TFIIH is a complex essential for transcription of protein-coding genes by RNA polymerase II, DNA repair of UV-lesions and transcription of rRNA by RNA polymerase I. Mutations in TFIIH cause the cancer prone DNA-repair disorder xeroderma pigmentosum (XP) and the developmental and premature aging disorders trichothiodystrophy (TTD) and Cockayne syndrome. A total of 50% of the TTD cases are caused by TFIIH mutations. Using TFIIH mutant patient cells from TTD and XP subjects we can show that the stress-sensitivity of the proteome is reduced in TTD, but not in XP. Using three different methods to investigate the accuracy of protein synthesis by the ribosome, we demonstrate that translational fidelity of the ribosomes of TTD, but not XP cells, is decreased. The process of ribosomal synthesis and maturation is affected in TTD cells and can lead to instable ribosomes. Isolated ribosomes from TTD patients show an elevated error rate when challenged with oxidized mRNA, explaining the oxidative hypersensitivity of TTD cells. Treatment of TTD cells with N-acetyl cysteine normalized the increased translational error-rate and restored translational fidelity. Here we describe a pathomechanism that might be relevant for our understanding of impaired development and aging-associated neurodegeneration.

Introduction

Trichothiodystrophy (TTD) is a developmental disorder with an eponymous skin and hair pathology, ichthyosis of the skin and brittle, sulfur deficient hair. Microcephaly, impaired intelligence, recurrent infections and retarded growth with short stature are often accompanied by the development of cataracts (1). These symptoms are shared with the progeroid syndrome Cockayne (CS) that shows additional features of the aging body like alopecia, retinal degeneration and cachexia (2). Severe cases of both syndromes can lead to childhood death. 50%; of TTD cases share ultraviolet (UV)-sensitivity of the skin with CS, as mutated genes that can cause these disorders are active in the repair of UV-induced deoxynucleic acid (DNA)-lesions of the skin. Thus TTD and CS are commonly attributed DNA-repair disorders (3). However, accumulating DNA damage might not be the underlying pathomechanism since CS and TTD are cancer-free and furthermore 50%; of TTD cases do not show DNA-repair defects (4,5). Total loss of the affected DNA repair pathway nucleotide excision repair (NER) is followed by the severe cancer-prone skin disorder xeroderma pigmentosum (XP). In contrast, XP does not display the drastic childhood developmental impairments of CS and TTD. Therefor alternative explanations for the severe phenotype of CS and TTD are discussed (6). Mutations in TFIIH can cause all these syndromes and combinations thereof, thus it is challenging to unequivocally identify underlying pathomechanisms. TFIIH initiates ribonucleic acid (RNA) polymerase II transcription on every protein-coding gene and TFIIH mutations disturb this process, therefor CS and TTD might be transcriptional syndromes (7–11). One alternative function of TFIIH is it's essential role for transcription by RNA polymerase I. RNA polymerase I synthesizes the functional and structural backbone of the ribosome (12–14). Ribosomal biogenesis is an intense energy consuming process (60%; of total transcription) and 50%; of all RNA polymerase II transcription occurs on genes coding for ribosomal proteins (15). Recent publications could unravel severe disturbances in ribosomal biogenesis and maturation in CS (16–20) as well as in TTD (14,21) leading to a loss of protein homeostasis (proteostasis) (22,23). Loss of proteostasis characterizes aging-associated neurodegenerative syndromes (24) and thus might cause the neurodevelopmental/neurodegenerative symptoms in TTD and CS. This hypothesis is supported by the newly identified TTD mutations in tRNA synthetases which are essential for proper translation and hence, for balanced protein homeostasis (5,25). Recently Phan *et al.* could show that TFIIE mutation, causing a DNA-repair proficient form of TTD, severely affects ribosomal maturation leading to translational infidelity of the ribosome and disturbances in proteostasis (21). This pathomechanism has already been described for CS (22,23) and as TFIIH mutations can cause TTD as well as CS, we asked the question if this pathomechanism might also be at play in cells of TTD patients suffering from TFIIH mutations. Using patient cells with a broad variety of mutations in TFIIH, we can show that TTD, but not XP mutations affect the ability

Received: August 23, 2022. **Revised:** October 11, 2022. **Accepted:** October 25, 2022

of the ribosome to translate oxidatively damaged mRNA and are accompanied by a loss of proteostasis.

Results

Loss of proteostasis characterizes cells from TTD patients

Mutations in three subunits of TFIIH can cause TTD. In an attempt to identify the common underlying pathomechanism of TTD, we studied five TTD patient-derived fibroblast strains covering the whole spectrum of TFIIH/TTD mutations. Two of the TTD patient cell strains were transformed by SV40 ($p8^{Mut}$ or XPD^{Mut}) and three primary strains with the indicated mutant subunit (TTD/p8, TTD/XP-B, TTD/XP-D) were investigated. The transformed cells were subject to mutational analysis and reconstituted with wildtype XPD or p8, respectively, ($p8^{Rec}$orXPD^{Rec}) (Supplementary Material, Fig. S1). The reconstitution did only partially overcome the functional deficits as shown by the intermediate UV-sensitivity of p8 reconstituted cells (Supplementary Material, Fig. S1D). Additionally, two XP-patient derived strains with mutations in XPD showing no TTD features were utilized. As controls served a transformed wildtype fibroblast line (ctr) and untransformed primary fibroblasts (C3PV) (Supplementary Material, Table S1). Western blot analyses of three TFIIH subunits (Fig. 1A and B) showed that TTD mutations can de-stabilize the TFIIH complex as previously reported (26,27). To investigate if these cells display a stress-sensitive proteome, we prepared cytoplasmic extracts, removed insoluble proteins by ultracentrifugation and challenged the proteome with heat and urea stress. A short heat treatment followed by centrifugation and quantification unraveled a high level of thermal instability in TTD cells that could only partially be rescued by the reconstitution of the transformed cell strains (Fig. 1C, left). In contrast, the proteome from a XP-XPD patient showed no elevated heat instability (Fig. 1C, left). Urea is a strong chaotropic reagent and incubation with 2 M urea was used to expose hydrophobic side chains that can be quantified by BisAns-flourescence. Stability of the proteome against stressors like heat treatment or urea are hallmarks of long-living species (28) and are strongly reduced in the primary TTD cells and in the transformed $p8^{Mut}$ cells. Extracts from the transformed XPD^{Mut} cells did, in contrast to the thermal instability, not display elevated unfolding by urea (Fig. 1D). However, the overall reduced proteotoxic stress resistance in TTD cells is a sign for a loss of proteostasis. Hypothesizing that this proteostatic imbalances might origin from a disturbed protein translation process, we quantified ongoing translation by o-propargyl-puromycin (OPP) incorporation in the growing amino-acid chains. Puromycin leads to an interruption of translation and the quantification of incorporated puromycin by fluorophore-labeled OPP revealed an elevated translational activity in all primary TTD cells in contrast to XP cells (Fig. 1E, right). The transformed strains did not show significant aberrations in translation when compared to the wildtype strain (Fig. 1E, left). Total protein synthesis measured by 35S-methionine incorporation in the proteome was not found to be upregulated in all TTD cells (Supplementary Material, Fig. S2D). This suggests that translation is not always leading to successful protein synthesis and might point toward a qualitatively disturbed translation process at the ribosome as, using these assays, already observed in TFIIE mutant cells (29). Proliferation kinetics with all cell lines revealed a severely retarded growth of all patient cells (Fig. 1F). In the case of the TTD–XPB cells the proliferation was so slow that this strain could only be used for assays that did not require high amounts of cells. Taken together we observed an elevated proteome instability and disturbances in protein synthesis leading to a loss of proteostasis in TFIIH mutant TTD cells.

Error-prone translation process in TTD cells

Translational fidelity of the ribosome is a parameter distinguishing short- from long-living species (30) and differs significantly between mice and humans (22). We addressed the question if the observed decline in stress resistance of the TTD proteome could be due to a globally enhanced error rate of the translation process. We took advantage of a well-established technique using luciferase-reporter genes with defined mutations (31). The mutations inactivate the luciferase, and when translated correctly, no luciferase activity can be measured. However, when translated incorrectly luciferase activity is detected and indicates an error-prone translation process at the ribosome (Fig. 2A) (Supplementary Material, Fig. S4A). When transfected with a plasmid encoding luciferase with a mutation altering a lysine to an asparagine residue (K529N), TTD patient cells, but not controls or the two XP cells, were found to re-activate erroneously the firefly luciferase indicating an inaccurate translation process (Fig. 2B) (Supplementary Material, Fig. S4B). As the luciferase-plasmid transfection method does not discriminate between errors during transcription by RNA polymerase II and translation at the ribosome, we synthesized luciferase encoding mRNA in vitro and transfected this mRNA into the cells. By this method we omitted the cellular transcription apparatus and directly assessed translation at the ribosome. In fact, when transfected with mRNA encoding mutant firefly, all different TTD cells, but not XP or control cells, display elevated luciferase activity indicating translational infidelity of the ribosomes (Fig. 2C). These results strongly support the hypothesis that the quality of the translation process at the ribosome is disturbed in TFIIH mutant TTD cells. To mimick the mutation of the TTDA protein, we reduced the expression of TTDA by siRNA treatment in control fibroblasts and monitored translational fidelity. In fact, knockdown of TTDA induced translational infidelity as demonstrated in Fig. 2D. This experiment causally revealed that the presence of the entire TFIIH complex is necessary to maintain the quality of protein synthesis.

Processing of the pre-rRNA and subunit stoichiometry of the ribosome can be affected by TFIIH-mutations

TFIIH plays a role as an elongation factor of RNA polymerase I (13,14), thus we wondered if TTD/TFIIH mutations affect pre-rRNA synthesis and processing. Interestingly, only p8 mutated TTD cells display clear reductions in pre-rRNA synthesis, measured by qPCR. (Supplementary Material, Fig. S2A–C). However, evidence from the group of Giglia-Mari (14) and a recent publication (21) suggests that one common disturbance in TTD might be a maturation defect of the pre-rRNA. Following this hypothesis we performed Northern blot analysis to visualize and quantify the intermediates of the pre-rRNA processing (Fig. 3A). As shown in Fig. 3B and C maturation is affected in most, but not all TTD cells, as revealed by a reduced 41S/47S ratio and an accumulation of later processing intermediates. In contrast, XP cells showed an elevation of all processing intermediates. The purification of ribosomes involves a sucrose-cushion centrifugation under high-salt conditions (32). As described in previous studies, ribosomes from TFIIE-mutant TTD cells (21) and from CS cells (23) are not stable under these conditions. To investigate if this holds true for TFIIH-mutant TTD ribosomes, cytoplasmic extracts from transformed TTD cells were isolated and ultracentrifuged at

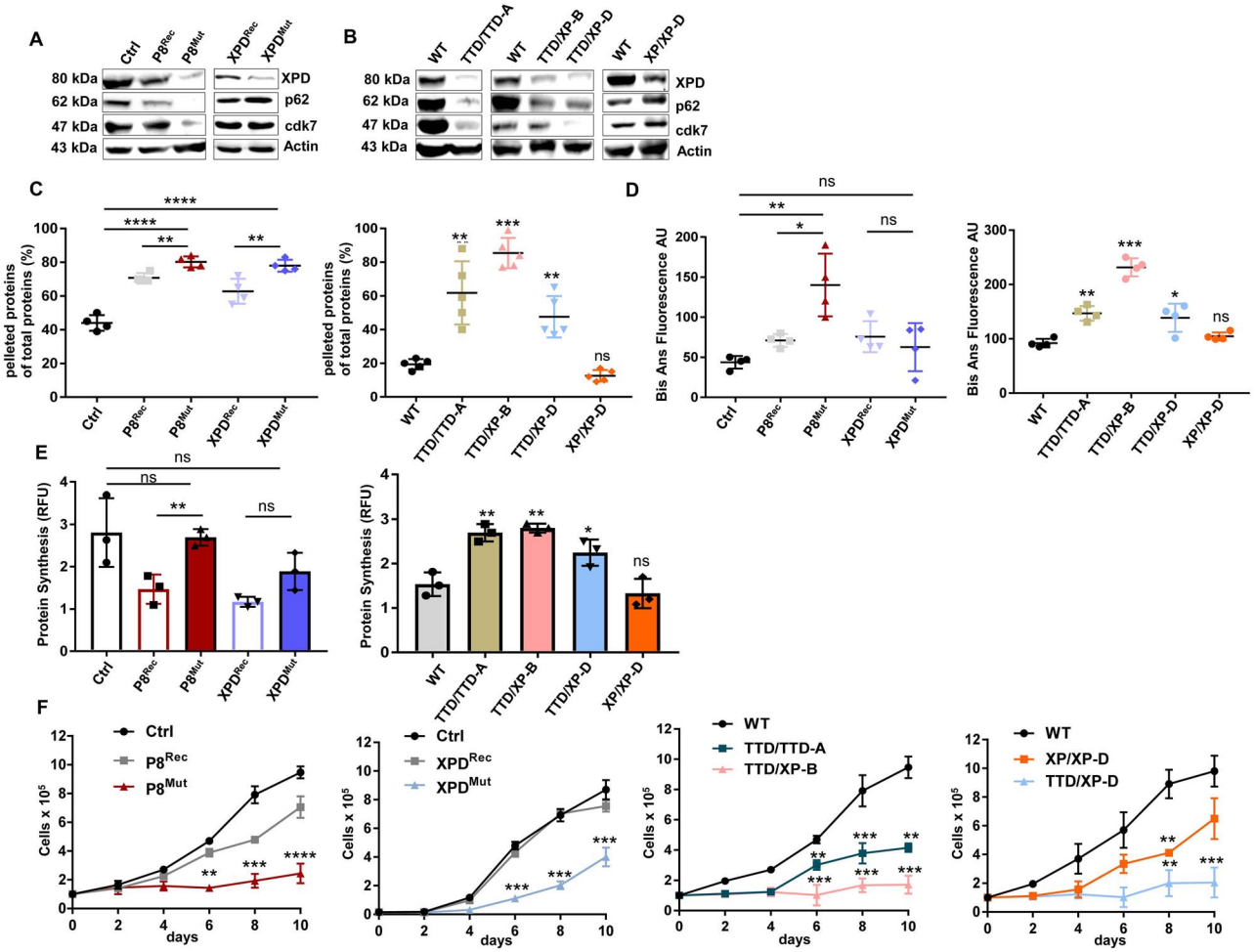

Figure 1. Imbalanced protein homeostasis and reduced growth rate in TFIIH mutant TTD cells. (**A**) Western blot analysis of the selected TFIIH subunits XPD, p62 and cdk7 in whole cell lysates of TTD cells. Transformed cell lines were Control (1306 fibroblasts), $P8^{Rec}$ (TTDA transfected with wt P8), $P8^{Mut}$ (TTDA), XPD^{Rec} (XPD transfected with wt XPD) and XPD^{Mut} (TTD2GL). Actin was used as a loading control. The cells used for this study are listed in Supplementary Material, Table S1. (**B**) TFIIH subunit abundance in primary fibroblasts from TTD and XP cells and healthy wild type C3PV cells used as control**.** Actin served as loading control in western blots. (**C**) Heat sensitivity analyses of cytoplasmic extracts in control, TTD and XP cells shows increased percentage of pelleted proteins in all TFIIH mutant TTD cells after heat treatment for 15 min at 99°C when compared to controls. (**D**) Protein stability was measured in control, TTD and XP extracts after denaturation with 2 M urea (2 h) and labeling with BisANS dye. Fluorescence intensity of BisANS was measured at 500 nm after excitation at 375 nm. (**E**) Protein synthesis analyses in control, TTD and XP cells by using five FAM-Azide detection of OPP-labeled proteins shows increased translation in all TFIIH mutant TTD cells. (**F**) Proliferation kinetics of TTD and XP cells compared to control cells indicates reduced cell proliferation in all patient-derived cells. Values are represented as mean ± SD of at least three independent experiments. Asterisk (*) in the figure represent (*$P < 0.05$, **$P < 0.01$, ***$P < 0.001$, ****$P < 0.0001$).

110 000 g. Subsequently, the pelleted ribosomes were dissolved and subjected to mass spectrometric analysis. When the relative abundance of ribosomal proteins was compared with reconstituted controls, the $p8^{Mut}$ ribosomes display a general underrepresentation of ribosomal proteins of the small subunit (Fig. 3D and E). This is in line with the observation that the mature 18S rRNA, backbone of the small subunit, was found to be reduced in p8 mutated TTD cells (Supplementary Material, Fig. S2C). However, the analysis of ribosomal protein abundance in isolated XPD^{Mut} ribosomes displayed no significant aberrations as depicted in the volcano blot of Fig. 3E. Interestingly, western blot analysis with $p8^{Mut}$ cells revealed that the ribosomal proteins are present in whole-cell lysates but are underrepresented in the purified ribosomes (Fig. 3F, left panels; Supplementary Material, Fig. S3A). This can indicate an instable assembly of the small subunit of the ribosome as already shown for ribosomes isolated from CS and TFIIE/TTD patient cell lines (21,23). The ribosomes from the transformed XPD–TTD cells (XPD^{Mut}), in line with the mass spectrometric analyses, did not display significant aberrations (Fig. 3F, right panels; Supplementary Material, Fig. S3B). Taken together, p8 mutated TTD cells display disturbances in pre-rRNA synthesis and processing accompanied by a reduced assembling stability of ribosomal proteins of the small ribosomal subunit.

Translational infidelity in TTD is provoked by ROS

Next we were interested if we can detect translational inaccuracy in the reconstituted in vitro translation, following the protocol by Penzo *et al.* (32). Ribosomes were purified from cytoplasmic extracts by ultracentrifugation through a high-salt sucrose cushion and reconstituted with ribosome-depleted rabbit reticulocyte lysate (Fig. 4A). Strikingly, in the *in vitro* assay, purified ribosomes from TTD or XP patient cells did not display an elevated error-rate although the same mutant luciferase (MUT) mRNA was used that was error prone translated when transfected into the cells from which the ribosomes origin (Fig. 4B, compare with Fig. 2). These results imply that there are specific cellular conditions in TTD at

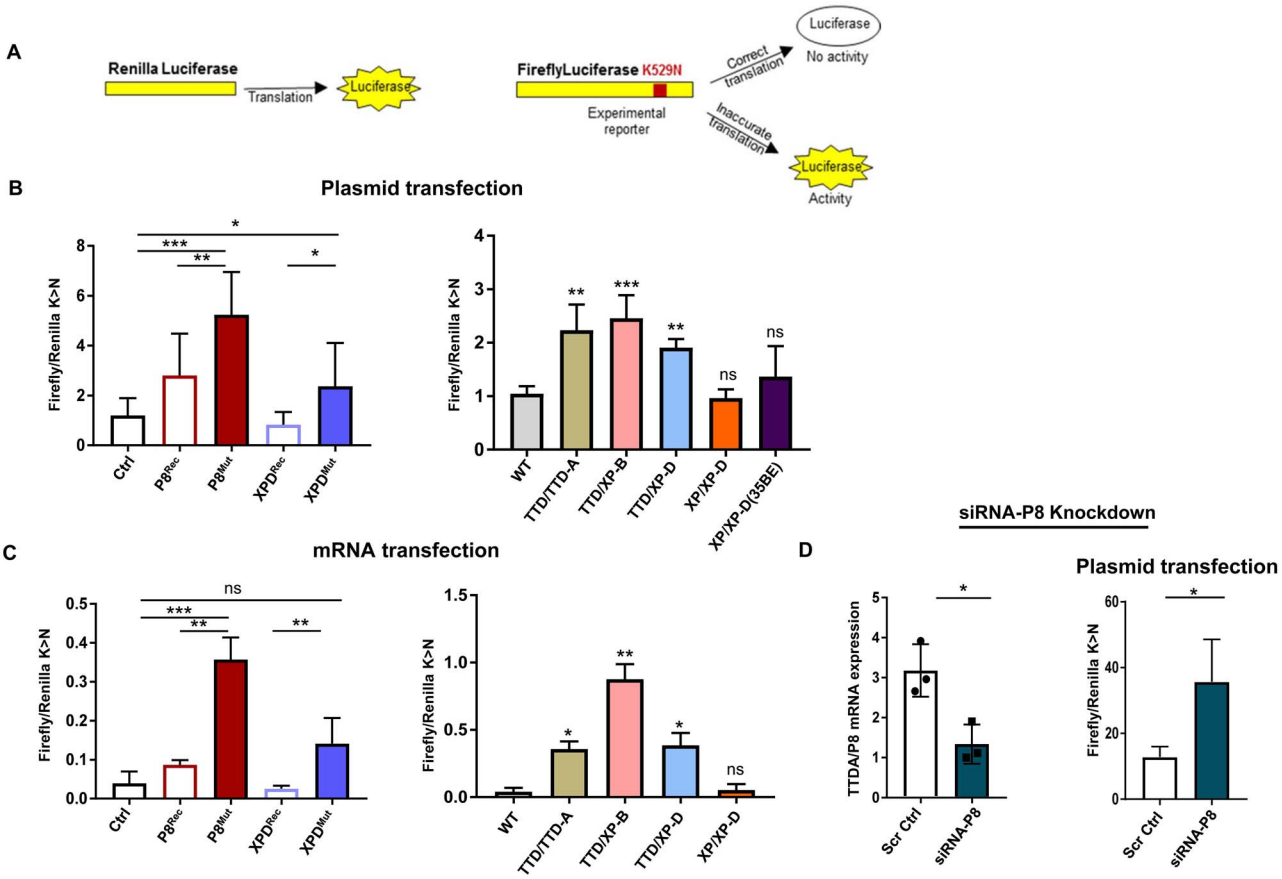

Figure 2. Translational inaccuracy in TTD cells. (**A**) Scheme of luciferase-based translation fidelity assay. Cells were transfected with a control reporter (renilla) in combination with three different firefly reporters: a PC with no mutation, a permanent inactivated NC and a point-mutated K529N firefly luciferase reporter (MUT). The point mutation inactivates the luciferase and by inaccurate translation the activity of the luciferase is reactivated. (**B**) Translation accuracy was measured in control (1306) or WT (C3PV), TTD and two XP cells by transfection (electroporation) of control or mutant firefly luciferase reporters, with a mutated lysine 529, determining the frequency of amino acid misincorporation. The principle of the assay is depicted in the scheme above. The activity of the luciferase was determined by luminescence measurement and normalized to the luminescence of renilla luciferase. (**C**) Plasmids encoding for renilla and firefly luciferases were transcribed to capped mRNAs by T7 polymerase. Reporter mRNAs were transfected (lipofectamine) in control, TTD and XP cells. (**D**) Knockdown of the TFIIH subunit p8 induces translational infidelity. A total of 72 h after siRNA transfection either mRNA was harvested and quantified (left) or the plasmid based translational fidelity experiment performed (right). Values are mean ± SD of three or more independent experiments. Asterisk (*) in the figure represent (*$P < 0.05$, **$P < 0.01$, ***$P < 0.001$, ****$P < 0.0001$).

play that are not mirrored in the *in vitro* assay. We now asked if DNA-damage signaling might contribute to translation infidelity of the ribosomes and challenged healthy primary fibroblasts with different genotoxic stressors. Subsequently we transfected the cells with mRNA encoding the positive control (PC) and MUT and monitored luciferase activity 24 h later (Fig. 4C, Supplementary Material, Fig. S5C). Indeed, when the cells were irradiated with 10 J/m^2 ultraviolet C (UVC), the accuracy of the translation process at the ribosomes was affected. Interestingly this elevated error rate was typical for UV-irradiation and could not be provoked by double-strand breaks created by etoposide treatment (Fig. 4C). This result suggests that UV-damage specific signaling affects the accuracy of the translation process. As UV-light induces reactive oxygen species (ROS) (33) and TTD cells are hypersensitive to oxidizing agents (34), we monitored by DCF fluorescence the levels of endogenous ROS. Interestingly, and in accordance with findings in CS (35), we found highly elevated levels of endogenous ROS in all patient cells, including XP (Fig. 4D, Supplementary Material, Fig. S5A). Speculating that cellular ROS might harm mRNA, we pretreated the *in vitro* transcribed mRNA with H_2O_2 and performed again the *in vitro* translations with patient ribosomes. As depicted in Fig. 4E (Supplementary Material, Fig. S5D) the ribosomes isolated from TTD, but not from XP cells, are not able to correctly translate oxidized mRNA, but are error-prone and are thereby reactivating luciferase activity. These results clearly show that the ribosomes from TTD patients display intrinsic functional deficits. Interestingly ribosomes isolated from CS-cells did not show an increased translational infidelity when challenged with oxidized mRNA thus proving the specificity of this defect for ribosomes purified from TTD cells (Fig. 4F). To investigate if we find signs of oxidized RNA in urine samples of TTD patients and their relatives, an 8-oxo-guanosine ELISA was performed. Indeed, in the TTD cases a highly significant elevation of oxidized RNA products could be detected, indicating that oxidized RNA might play a role in the disease (Fig. 4G).

Rescue experiments with anti-oxidant and pharmaceutical chaperones

In an attempt to reduce cellular ROS we pre-treated TTD cells with the anti-oxidant N-acetyl-cysteine (NAC), and subsequently performed a translation accuracy test transfecting mRNA. As shown in Fig. 5A, a 24 h treatment with 1 mM NAC significantly reduced the error-rate of the translation machinery of TTD cells. This result demonstrates that in fact cellular ROS contributes to the

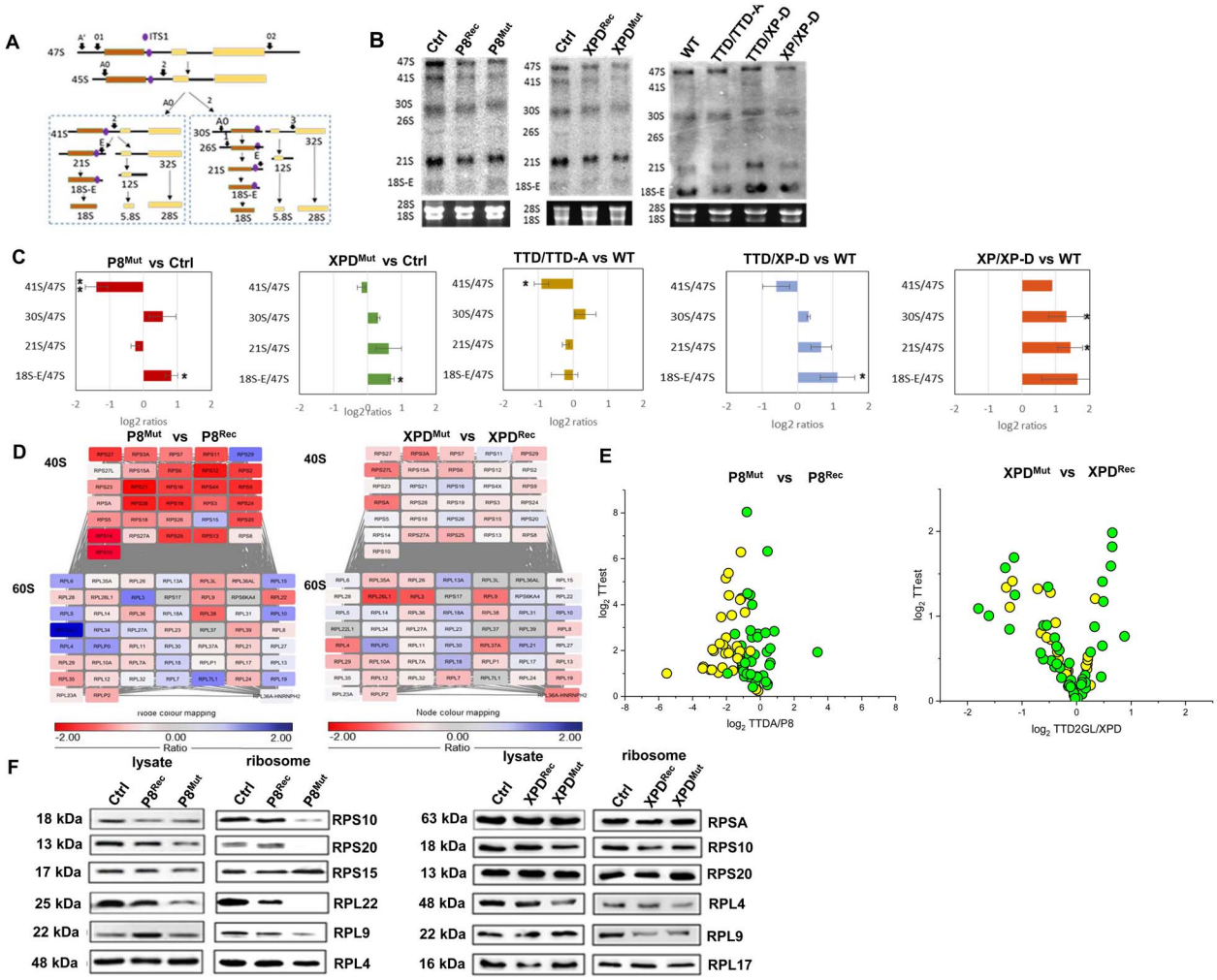

Figure 3. Disturbed pre-rRNA processing and ribosomal composition in TTD cells. (**A**) Scheme of the rRNA processing pathway in human cells, adapted from Mullineux and Lafontaine (2012). The ITS1 probe is identified in purple. (**B**) Representative northern blots of control (1306) or WT (C3PV), transformed and primary TTD and XP cell lines incubated with ITS1 probe. (**C**) RAMP profiles (Ratio Analysis of Multiple Precursors) of northern blots in (B). (**D**) Mass spectrometric analysis shows a non-significant decreased amount of ribosomal protein of the small 40S ribosome subunit and a non-significant increased amount of ribosome protein of the large 60S ribosome subunit. Signal intensities of isolated ribosomes of (Left) transformed TTD cells $P8^{Rec}$ (TTDA transfected with wt P8), $P8^{Mut}$ (TTDA) and (right) XPD^{Rec} (XPD transfected with wt XPD) and XPD^{Mut} (TTD2GL). Representation of each ribosomal protein color coded with under-represented (red), normal (white) and over-representation (blue). (**E**) Quantification of mass spectrometric data by Volcano plot shows a non-significant reduction of ribosomal proteins of the small 40S subunit and a non-significant increase in ribosomal proteins of the larger 60S subunit in TTD cells compared to reconstituted cells. (**F**) Western blot analysis of selected ribosomal proteins and of whole cell lysates of TTD mutated reconstituted and control cells. GAPDH was used as a loading control. Quantifications are given in the Supplementary Material, Figure S3. Values are mean ± SD of three or more independent experiments. Asterisk (*) in the figure represent (*$P < 0.05$, **$P < 0.01$, ***$P < 0.001$, ****$P < 0.0001$).

increased infidelity of translation. Pharmaceutical chaperones like tauroursodeoxycholic acid (TUDCA) and 4-phenylbutyric acid (4-PBA) are able to overcome ER-stress mediated apoptosis and restore proliferation in CS-cells (22,23). To investigate if these compounds of low toxicity also impact on parameters of ribosomal biogenesis in TTD cells, rescue experiments with TUDCA were performed. Strikingly, treatment with TUDCA normalized RNA polymerase I transcription, reduced protein synthesis and the accumulation of processing intermediates of the primary transcript (Fig. 5B–D). Moreover, pharmaceutical chaperone treatment stimulated markedly the proliferation of p8 mutant cells (Supplementary Material, Fig. S6). These experiments suggest that the tested parameters of ribosomal biogenesis and performance are affected by proteotoxic stress that is dampened by TUDCA. Moreover, these experiments provide the base for a causal treatment of TTD with drugs that are approved for human intervention.

Discussion

This study is based upon the assumption that diseases with multigenetic origin like TTD are caused by a shared cellular pathomechanism that determines the common phenotypical symptoms on the organismal level. In a recent publication Phan *et al.* described that TFIIE mutations, leading to TTD, impact on RNA polymerase I transcription, processing and pre-ribosomal maturation resulting in an error-prone translation process and a loss of proteostasis (21). Here we addressed the hypothesis that mutations in TFIIH might also disturb ribosomal performance and proteostasis. In consequence, we speculate that ribosomal dysfunction might be the underlying cellular pathomechanism in TTD. In support of this hypothesis, ribosomal performance is significantly affected by all TTD mutations in TFIIH, specifically impairing the proper translation of oxidized mRNA and accompanied by a reduced stress resistance of the proteome.

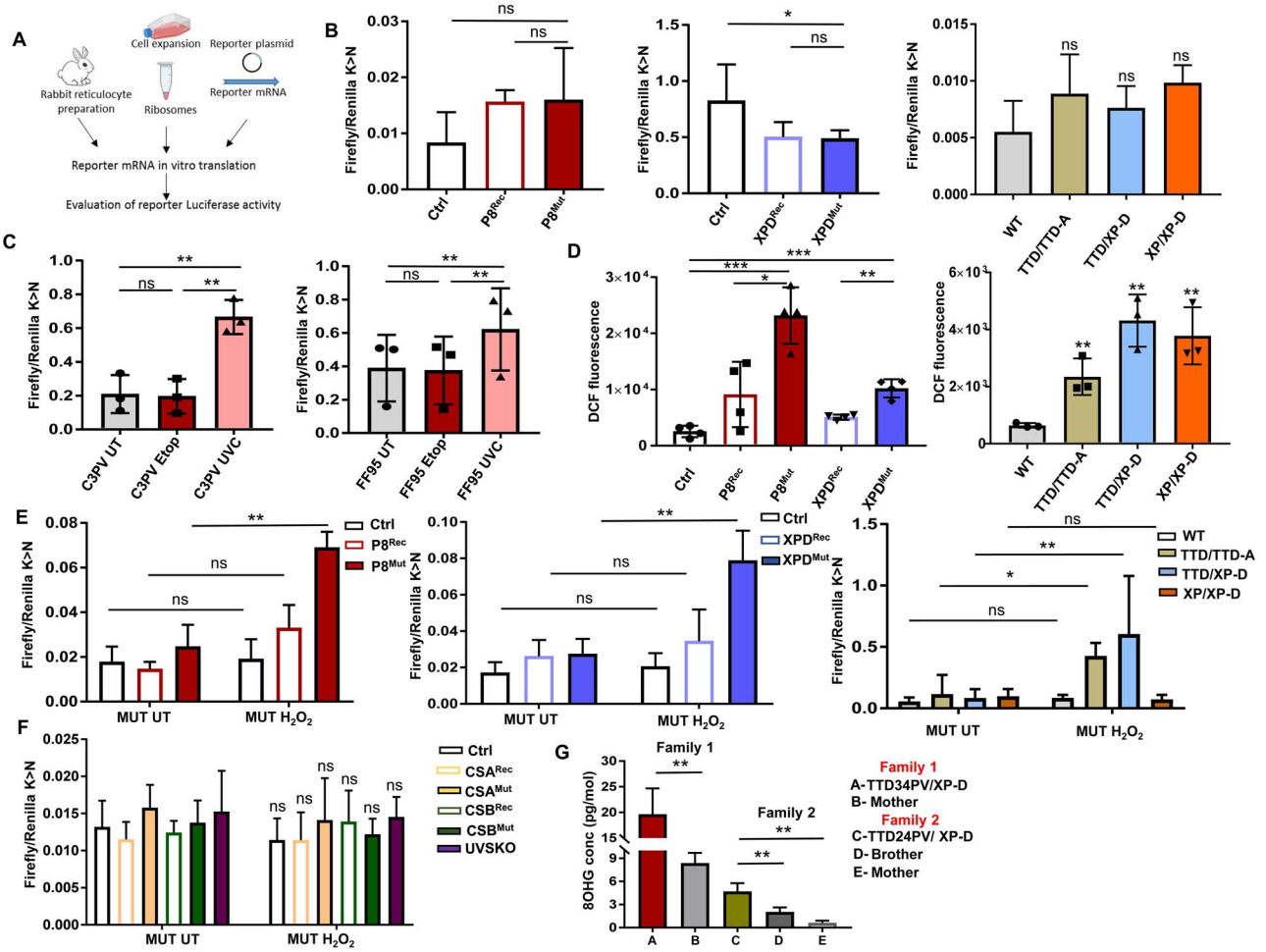

Figure 4. Oxidized mRNA is erroneously translated by TTD ribosomes. (**A**) Representative scheme of reconstituted *in vitro* translation. (**B**) *In vitro* translation was performed according to the protocol of Penzo *et al.* (32) with isolated ribosomes from all different patient and control cell lines. No significant differences were seen in TTD nor in XP cell lines. (**C**) Transfection of control fibroblast cell lines from healthy donors with firefly mutant mRNA showed increased translational infidelity in both control cells (C3PV and FF95) after irradiation with UVC (10 J/m^2) but not after Etoposide treatment. Paired *T* test was used for analysis. (**D**) Intracellular ROS levels were assessed by DCFH oxidation-sensitive fluorescent dye in control, TTD and XP cells. Fluorescence values were detected by flow cytometry and indicate higher ROS in all TFIIH mutant cells as compared to healthy wild type cells. (**E**) *In vitro* translation was performed with isolated ribosomes from above mentioned cell lines with *in vitro* oxidized mRNA (100 uM H_2O_2 for 45 min) and showed increased translational infidelity in all TFIIH mutant TTD cells as compared to control and XP cells. (**F**) Isolated ribosomes from Cockayne syndrome cell lines were tested in *in vitro* translation with oxidized mRNA (100 uM H_2O_2 for 45 min). The experiments showed no changes in translational infidelity in CS cells as compared to their reconstituted controls. (**G**) Urine samples of two TTD patients and their families were analyzed by ELISA, quantifying the oxidized mRNA indicator 8oxoG. Values are mean ± SD of three or more independent experiments. Asterisk (*) in the figure represent (*$P < 0.05$, **$P < 0.01$, ***$P < 0.001$, ****$P < 0.0001$).

However, the hitherto analyzed parameters of ribosomal biogenesis are not deviant in all TFIIH/TTD cell strains. The transformed XPD cell strain showed high translational infidelity in all assays but did not display pre-rRNA maturation defects nor ribosomal instability, suggesting that we are still ignorant about the exact origin and nature of the molecular defect in ribosomes that causes translational infidelity. The fact that UV-irradiation impacts on translational fidelity of the ribosomes could imply that the ribosome itself is damaged by the UVC treatment. Induced reactive oxygen species as a side effect of UVC treatment are not sufficient to explain the elevated translational error rate in UV-treated wild-type cells or in TTD, as ROS levels are also found to be high in the XP cells without inducing translational infidelity. Therefor we assume that disturbances in ribosomal biogenesis that are apparent in TTD, but not in XP, are resulting in ribosomes that are not able to cope with an elevated load of oxidized mRNA. Oxidized mRNA, that might be also present in the tested XP cells displaying highly elevated ROS levels, might not trigger translational fidelity and proteostasis imbalance without a 'second hit' at the ribosome.

The description of tRNA synthetases being mutant in TTD cases (5,25) further supports our hypothesis of a failure in protein synthesis as the common motive in TTD. Editing-defective tRNA synthetases have been shown to cause protein misfolding and in consequence neurodegeneration (36). Lee *et al.* showed that disruption of translational fidelity in neurons lead to the accumulation of misfolded proteins and cell death. Therefor we speculate that the neurodevelopmental/neurodegenerative traits of TTD and CS are provoked by a reduced ribosomal fidelity that might not cause problems to fibroblasts but might be detrimental for neurons. Cells from CS and TTD patients are hypersensitive to oxidizing agents and undergo apoptosis after oxidative challenge (34,37,38). The trigger could be DNA-oxidation (39), protein oxidation, as shown for CS cells (22), or RNA oxidation as firstly characterized in this study. RNA oxidation does induce translational

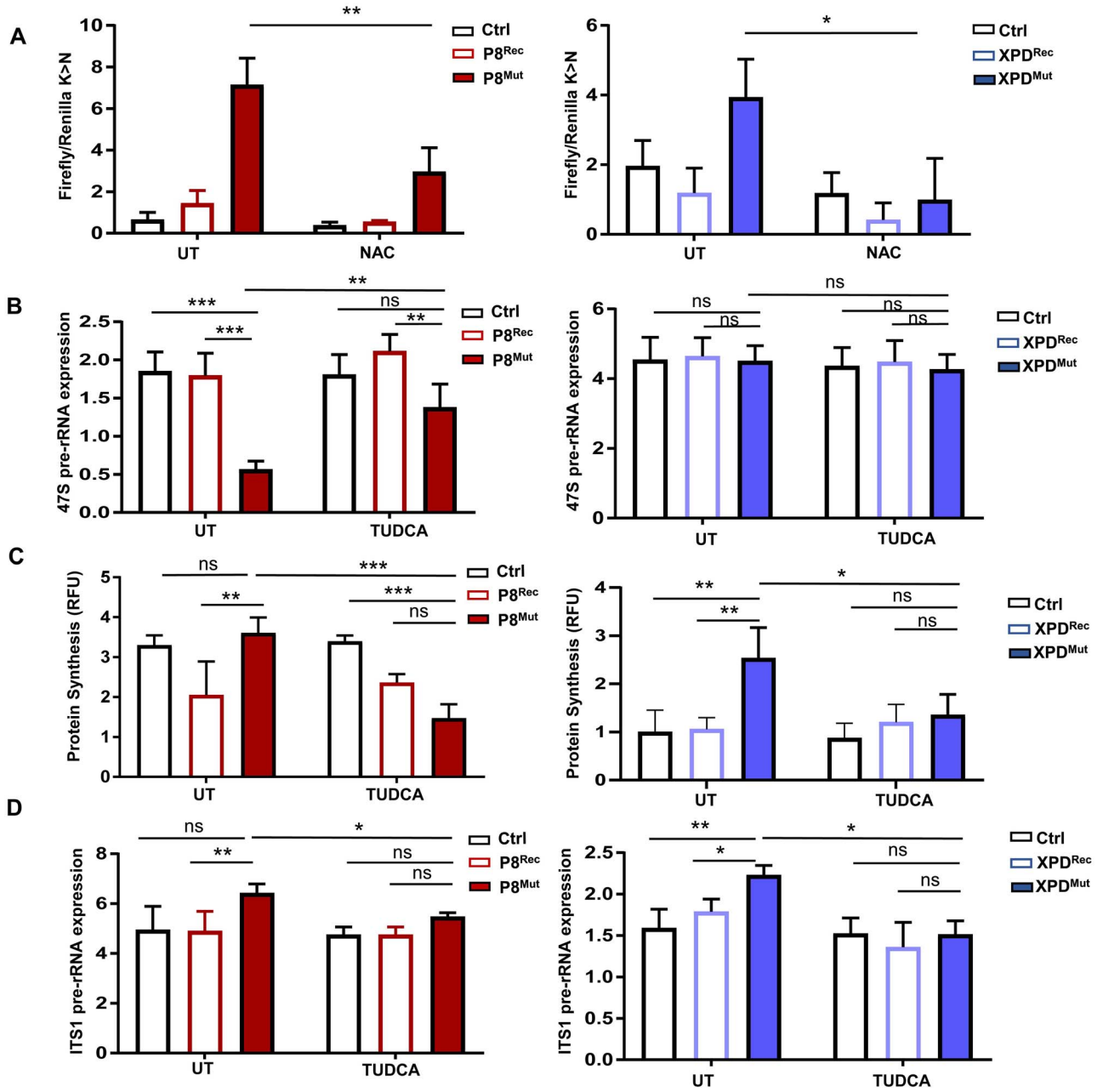

Figure 5. Rescue experiments with N-acetyl-cysteine and the pharmaceutical chaperone TUDCA. TUDCA restores RNA polymerase I transcription, rRNA processing and protein synthesis in TTD cells. (**A**) Plasmids encoding for renilla and firefly luciferase were transcribed to capped mRNAs by T7 polymerase. Reporter mRNAs were transfected (lipofectamine) in the transformed TTD cell lines $P8^{Mut}$, $P8^{Rec}$, XPD^{Mut} and XPD^{Rec} pretreated with 1 mM N-acetyl-cysteine for 24 h. (**B**) 24 h pre-treatment of p8- and XPD-mutated cells with TUDCA (200 μM) followed by quantitative PCR analysis of 47S pre-rRNA expression. (**C**) Protein synthesis analysis after TUDCA treatment. (**D**) Reduction of processing defects measured by ITS1 accumulation by 24 h treatment with TUDCA (200 μM). Quantitative PCR analysis of the ITS1 region. Values are represented as mean ± SD of at least three independent experiments. Asterisk (*) in the figure represent (*$P < 0.05$, **$P < 0.01$, ***$P < 0.001$, ****$P < 0.0001$)

infidelity (40) and here we describe the unfortunate combination of elevated ROS-levels and susceptible ribosomes that result in a loss of proteostasis. Loss of proteostasis, detected by a reduced stress-resistance of the proteome is a hallmark of CS-cells, distinguishes CS from the control UVs cells with the same defect in NER, (22,23) and here we show that it also separates TTD cells from XP cells. This suggests that loss of proteostasis is a common pathomechanism in both developmental/degenerative childhood disorders. Additionally, the observed loss of proteostasis might not origin from DNA damage, as the DNA-repair deficient XP patient cells do not display this imbalance. Neurodegenerative diseases are characterized by severe disturbances in proteostasis (41) and thus we speculate that the neurodevelopmental/−degenerative features of TTD and CS disease can be explained by a severe cellular failure in protein homeostasis. Proteome stability is a hallmark of long-living species (28,42) and thus it is conceivable that pathomechanisms that impact on proteome stability also impact on lifespan as displayed in the childhood diseases CS and TTD. Heat-stress resistance as a parameter of proteome stability can be improved in metazoans by a hyperaccurate mutation in the ribosomal protein RPS23. This mutation in the decoding center of the small subunit of the ribosome improves stop-codon readthrough

and significantly prolongs lifespan in all tested model organisms (43). This seminal study proves that the accuracy of the translation process at the ribosome impact on longevity as already implied by the fact that translational accuracy co-evolved with longevity in rodents (30). In a recent study, Shcherbakov *et al.* could convincingly show that reducing systemically translational fidelity of the ribosome by an amino-acid exchange in the protein of the small subunit RPS9 reduced life span and induced premature aging in mice (44). Translational infidelity has been shown in a variety of diseases: chronic lymphocytic leukemia (45), dyskeratosis congenita (46) and Diamond-Blackfan anemia (47). The broad variety of the phenotypes with cellular translational infidelity suggests that there might be cell-type specific mechanisms at play that are hitherto poorly understood. However, aging and premature aging are accompanied by a loss of proteostasis (24) and ribosomal accuracy might decline during lifetime in long-living organisms. This might be due to an age-related fading in the accuracy of ribosomal biogenesis itself.

Here we provide first molecular evidence that translational fidelity in TTD can be restored by treatment with N-acetyl-cysteine, a drug with low toxicity and side effects even at high doses (48), offering a treatment opportunity for the affected children. Moreover, a possible combination with TUDCA, often used as a dietary supplement, might open up novel horizons for this hitherto incurable disease.

Material and Methods

Cell culture

SV40-transformed human fibroblasts (1306, $P8^{Rec}$,$P8^{Mut}$,XPD^{Rec}, XPD^{Mut}) and primary human patient fibroblasts (TTD-P8, TTD-XPD, TTD-XPB and XP-XPD were cultured under conditions of 37°C, 5%; CO_2 and 3%; oxygen in DMEM (GIBCO) supplemented with 10%; fetal bovine serum (FBS, Biochrom), 2 mM L-glutamine, 100 U/ml penicillin and 100 μg/ml streptomycin (Merk Millipore). Reconstituted cells $P8^{Rec}$ and XPD^{Rec} were grown in the presence of Geneticin (200ug/ml). (Identification of cell lines in Supplementary Material, Table S1).

RNA isolation and cDNA synthesis

RNA isolation was performed using RNeasy Mini Kit (QIAGEN GmbH, Hilden, Germany) according to the manufacturer's description and harvested RNA measured by Nanodrop.

1 μg of RNA was pre-incubated with 250 ng of random hexamer primer $p(dN)_6$ in nuclease free water and incubated 5 min at 70°C. The reaction mix was, 4 μl of 5x M-MLV reverse transcriptase buffer, 1 μl M-MLV (400 U/μl) (Promega) and 0,5 μl RNasin (40 U/μl) (Promega) and supplemented with nuclease-free water to 20 μl. Reverse transcription was performed for 1 h at 37°C.

Real-time qPCR standard curve analysis

A total of 100 ng cDNA and FastStart Universal SYBR Green Master (04913850001, Roche Diagnostics) (denaturation at 95°C for 10 s, annealing at 60–68°C for 30 s, elongation at 72°C for 30 s) were used. A standard curve for the oligonucleotide of interest with linear regression with R^2-values > 0.8 was used for calculation of the absolute amount (ng) of the oligonucleotide of interest within 100 ng total cDNA. Primers used for the analysis of qPCR are listed in Supplementary Material, Table S3.

Ribosome isolation

Isolation of ribosomes was performed according to Penzo (32).

Carbonylation assay

Protein Carbonylation Assay Kit (Abnova) was used to quantify carbonylation. Cells were lysed in 1× complete lysis mix (10%; Glycerol, 1%; Triton X100, 137 mM NaCl, 20 mM Tris) pH 8.0, 2 mM EDTApH 8.1. Samples were centrifuged for 20 min (13 000×*g*) and the supernatants diluted adjusted to 10 mg/ml and incubated with 2,4-Dinitrophenylhydrazine (DNPH) (1/3v 6 M) for 10 min and further precipitated with (1/10v) 100%;TCA. After centrifugation for 2 min at 13 000×*g* the pellets were washed with acetone followed by solubilization in 200 μl 6 M guanidine. The OD was measured at 375 nm. The values were normalized according to the protein content, measured by BCA assay.

ROS measurement by FACS

For ROS cells were stained for 15 min with the fluorescent dye CM-H_2DCFDA 1 μM (DCF, Invitrogen) or 10 μM dihydroethidium (DHE, Invitrogen) in PBS. Cells were washed and harvested in 0.5 mL FACS buffer (PBS with 0.5%; FBS) and vortexed. Fluorescence was measured by FACS Canto II (BD Biosciences).

BisANS assay

Cells were harvested in TNE buffer (50 mM TrisHCl, 100 Mm NaCl, 1 mM EDTA, sonicated (3 × 30 s) and centrifuged for 20 min at maximum speed in a table-top centrifuge. Protein concentration of the supernatant was measured using Bradford assay. 100 μg of protein was incubated in 2 M urea for 2 h. BisANS was added (30 μM final concentration) and fluorescence was measured using an excitation wavelength of 375 nm and 500 nm emission. To assess ribosomal protein folding stability, 10 μg of isolated ribosomes were used.

BisANS dye	**4,4′-Dianilino-1, 1′-Binaphthyl-5, 5′- Disulfonic Acid, Dipotassium Salt**
Labeling buffer	50 mM Tris HCl, 10 mM $MgSO_4$, adjust to pH 7.4

Transfection and luciferase assay (plasmids)

pGL3 wild-type luciferase plasmid, hypoxanthine-guanine phosphoribosyltransferase (HRPT) negative control, renilla luciferase plasmid and K529N (lysin AAA–Asn AAC) (49) mutant firefly luciferase plasmid were a kind gift from Andrei Seluanov (Vera Gorbunova) from University of Rochester. 10^6 cells were transfected 5 μg of firefly reporter plasmid and 0.1 μg of renilla luciferase via electroporation using the Neon™ Transfection System (MPK1096, Invitrogen) (1100 V, 20 ms and 2× pulses). Cells were plated in a 96 well plate (5×10^4 cells/well in 100 μl) overnight in OptiMEM (31985070, Gibco) (antibiotic free media). DualGlo Luciferase assay kit (E2920 Promega) to measure. Luminescence and the ratio of firefly to renilla was used as an indicator of translational fidelity.

Luciferase assay with mRNA transfection

The plasmids pCl-neo (Control) and pCl-neo (K529N) (kindly provided by Dr Markus Schosserer) encode for fusion proteins of renilla and firefly luciferase. Plasmids were transcribed to mRNAs by using Ampli Cap-Max T7 High Yield Messager Marker Kit (C-ACM04037, CellScript). A total of 10^5 cells/well in 100 μl culture medium were seeded in white 96-well plate and grown overnight. A total of 500 ng mRNA in 50 μl OptiMEM (31985070, Gibco) and 1 μl of Lipofectamine® MessengerMAX mRNA Transfection Reagent (LMRNA003, Invitrogen) in 50 μl OptiMEM were incubated for 10 min at RT. 100 μl of mRNA-Lipofectamine-OptiMEM mixture

were transferred to each well and incubated for 24 h. To analyze the transfected cells luminescence was measured using DualGlo Luciferase assay as above.

O-propargyl-puromycin (OPP)

Protein synthesis was assessed by using Protein Synthesis Assay kit (Cayman Chemical 601100). The OPP analog was used for labeling translating polypeptide chains and 5-FAM-Azide for the subsequent detection of OPP-labeled proteins. A total of 10^5 cells were cultivated in a 96-well plate overnight and centrifuged for 5 min at 400×*g*. OPP working solution (1:2500) was added and after incubation for 30 min at 37°C cells were centrifuged. Cell-Based Assay Fixative was added for 5 min at room temperature, centrifuged and washed. After 30 min incubation with 5-FAM-Azide Staining Solution and washing fluorescence was measured using a microplate reader Varioskan™ LUX using excitation 485 nm/emission 535 nm.

^{35}S Methionine labeling

A total of 5×10^4 cells per reaction were collected by centrifuging for 5 min at 3000 rpm followed by incubation at 37°C for 30 min in 100 μl methionine-free DMEM with 10%; FBS and 1%; penicillin–streptomycin. After this 10 μl culture medium with 10 μCi ^{35}S-labeled methionine/cysteine (10 mCi/ml, Hartmann analytics) was added and incubated for 1 h. Following centrifugation for 5 min at 3000 rpm, pellet was resuspended in 100 μl 1 mg/ml BSA. Then 1 ml of cold 10%; TCA was added, the reaction was vortexed and incubated on ice (1 h). The reaction was transferred onto glass fiber prefilters (Merck, APFC02500), washed with cold 10%; TCA and subsequently with cold 70%; ethanol. For 5 min glass fiber prefilters were air dried and the amount of incorporated ^{35}S-label was analyzed with 5 ml liquid scintillation cocktail Ultima Gold™ (6013329, PerkinElmer) by Liquid Scintillation Analyzer Tri-Carb 4910 TR (PerkinElmer).

Proliferation analysis

To evaluate the growth of cell lines, 2×10^5 cells were seeded in a six well culture dish. For each time point four dishes were detached using trypsin and counted using automated cell counter (DeNOVIX Cell Drop FL). Cells were counted every 48 h over a period of 10 days.

Heat sensitivity assay

Heat sensitivity assay was performed according to the method of Treaster *et al*. (28).

Western blot analysis

Western blots were performed as previously described (23,29).

Northern blotting

A total of 5 μg of RNA was diluted with 2× RNA loading dye (50%; formamide, 7.5%; formaldehyde, 1× MOPS, 0.5%; ethidium bromide) and denatured at 65°C for 15 min and placed on ice for 5 min. The samples were loaded on a 0.9%; agarose gel and run at 80 V for 3 h. Transfer of nucleic acids was performed by capillary blot. The nylon membrane (RPN303S, GE Healthcare) and whatman paper were wetted in 2× SSC buffer, and placed on top of the RNA gel in a reservoir of 20× SSC (3 M NaCl, 0.3 M Na citrate, adjust to pH 7). Approximately 6 cm of dry filter paper was stratified over the gel/membrane and a weight of 500 g was placed on top. The transfer occurred overnight. After air drying, the membrane was crosslinked with 2× 1200 J UVC (UV Stratalinker ™ 1800) and was pre-hybridized with buffer (50%; formamide, 0.1%; SDS, 8× Denhards solution, 5× SSC buffer, 50 mM NaP buffer, 0.5 mg/ml t-RNA) for 2 h at 65°C. The ^{32}P-labeled (T4 polynucleotide kinase) oligonucleotide probe was denatured at 95°C for 10 min and added. The probe was Incubated for 1 h at 65°C and then at 37°C overnight. The membrane was washed with wash buffer (2X SSC) the next day and exposed to X-ray films and quantified using Image Quant Software according to Wang *et al*. (2016). For rRNA processing pathway analysis probes binding to the region ITS1 (5′ GGGCCTCGCCCTCCGGGCTCCGTTAATGATC 3′) was used.

Mass spectrometric analysis

Mass spectrometry analysis of isolated ribosomes was performed by Core Unit Mass spectrometry and proteomics (CUMP) University of Ulm. Label-free quantification of data was analyzed using Excel and volcano plots were generated using software R studio.

In vitro translation

In vitro translation was performed according to the protocol of Penzo *et al*. (32). In brief, rabbit reticulocyte lysate (Promega L4151) was depleted from ribosomes after mixing with an equal volume of cold 3.2 mM $MgCl_2$ solution and 40%;v of 1.5 M sucrose/150 mM KCl solution and centrifugation at 140 000 g in a MLS50 rotor for 4 h (S140). The supernatant was complemented with hemin (Sigma Aldrich) (50 μM). To isolate translation-initiation factors, the pelleted ribosomes were suspended with salt-wash solution and adjusted to 0.5 M KCl by the stepwise addition of 4 M KCl and incubated on ice for 10 min. The ribosomes were pelleted by a 2 h centrifugation step at 170 000 g in a (TLA-100S/N 07U1825, Optima MAX) Rotor. The supernatant and the salt-washed fraction was aliquoted and frozen. For *in vitro* translation analysis, rabbit reticulocyte lysates (S140) and salt-wash fraction (SWF) were combined with ribosomes and mRNA. 300 ng RNA (WT/K > N mutant), 8.8 μl S140, 0.25 μl SWF and 2 μl TM buffer were mixed in a 1.5 mL tube. A total of 2 μl of the ribosomes were added with a concentration of 0.0625 pmol/μl, diluted with nuclease-free water. Samples were incubated at 30°C for 2.5 h on a thermomixer. Following incubation, they were transferred to a 96-well plate for luminescence measurements using Dual-Glo®Assay System (Promega).

SW-solution	**0.25 M sucrose, 0.1 mM EDTA, 1 mM DTT, 25 μM hemin, RNase-free water**
10× Translation mix buffer	152 mM HEPES pH 7.5, 900 mM KAc, 15 mM MgAc, 80 Mm creatine phosphate, 200 μg/ml creatine phosphokinase, 8 Mm ATP dipotassium salt, 480 μM GTP disodium salt, 200 μg/ml calf liver tRNA, 100 μM amino acid mix minus methionine, 2 mM spermidine, 16 mM DTT

8-OHG ELISA Materials:

ELISA was performed according to the manufacturer's protocol. A total of 96 well pate provided in the OxiSelect ™ Oxidative RNA Damage ELISA Kit (STA-325) was coated with 100 μl of 8-OHG conjugate (1 μg/ml) per well and was incubated overnight at 4°C on an orbital shaker. After washing blotting was performed with 200 μl of Assay Diluent/wel for 1 h at room temperature. Urine samples were diluted in Assay diluent (40 μl diluent + 10 μl

96-well Protein Binding plate	Cell BIOLABS, INC
Assay diluent	200 μl/well
10× Wash Buffer	1× (250 μl/well)
Substrate Solution	100 μl/well
Stop solution 50 ml	100 μl/well
8-OHG standard	2 μg/ml 8-OHG in 1xPBS
8-OHG conjugate (1 mg/ml)	1 μg/ml in 1xPBS

sample) and added to the conjugate coated plate. The samples were incubated for 10 min on an orbital shaker, 50 μl of diluted 8-OHG antibody (1:500) was added to each well, followed by an incubation for 1 h at room temperature on an orbital shaker followed by three times washing. 100 μl of 8-OHG secondary antibody (1:1000) was added for 1 h at room temperature on the shaker. After washing 3× with 1X Assay diluent, 100 μl of substrate solution (RT) was added. The developing varies from 2–30 min depending on the color change of the reaction. Stop solution was added and the OD was measured at 450 nm by using av spectrophotometer.

N-acetyl cysteine (NAC) treatment and translation fidelity

The cells were treated with the antioxidant NAC (1 mM) for 24 h and translational fidelity assay with plasmids and electroporation was performed as described above.

Chemical chaperone treatments

For chemical chaperones, cells were treated for 24 h with TUDCA (200 μM) (Tauroursodeoxycholic Acid, Sodium Salt Affiliate of Merck Darmstadt, Germany) 4PBA (1 mM) (4-Phenylbutyric acid Sigma-Aldrich, P21005) and were cultured under standard conditions at 37°C, 5%; CO_2 and 3%; oxygen in DMEM media.

siRNA knockdown

Preparation of siRNA solution

SiRNA oligonucleotide (Accell™ Human GT2H5–404 672 siRNA-SMART pool 20 nmol) ready to use RNAs were purchased from commercial vendors (Dharmacon ™ Horizon Discovery Biosciences Limited). The lyophilized tube containing siRNA was centrifuged to collect the pellet at the bottom of the tube. The pellet was resuspended in RNAase-free 1× siRNA Buffer to get the desired final concentration (for 20 nmol of siRNA and a 20 μM stock concentration, 1000 μl siRNA buffer was added). The solution was pipetted up and down five times, the tube was sealed securely and was placed on an orbital shaker for 30 min at room temperature. Resuspended siRNA was used immediately and the rest was aliquoted into smaller volumes and was stored at −20°C.

Delivery of siRNA into the cells

siRNA was delivered into the cells using electroporation. For this purpose C3PV (wild type fibroblasts) were grown in T75 flasks till they reached 75%; confluency. On the day of transfection, the cells were harvested, washed with PBS and were counted. 1×10^6 cells were harvested and transfected using via electroporation using Neon™ Transfection System (MPK1096, Invitrogen) with following parameters: 1400 V, 20 ms and 2× pulses. 2 μM of siRNA was used. Transfected cells were plated in 10 cm dishes (2×10^5 cells), and were allowed to grow for 24 h in reduced serum media (Opti-Mem) at 37°C, 5%; CO_2 and 20%; oxygen. The next day media was replaced with normal media in DMEM (GIBCO) media supplemented with 10%; fetal bovine serum (FBS, Biochrom), 2 mM L-glutamine, 100 U/ml penicillin and 100 μg/ml streptomycin (all from Merk Millipore). 72 h after transfection, the cells were collected for the desired experiments.

qPCR assay validation

The extraction of RNA was performed using RNeasy Mini Kit (QIAGEN GmbH, Hilden, Germany), according to manufacturer's protocol. The RNA was reverse transcribed using a random hexamer primer $p(dN)_6$. The cDNA was diluted 1:50 prior to performing qPCR analysis. The quantitative PCR reaction was performed using a 7300 Real Time PCR System (Applied Biosystems®, Life Technologies GmbH, Dramstadt Germany). The data to validate the knockdown of GT2H5 gene (P8/TTDA) was analyzed using 7300 Systems SDS software.

Luciferase plasmid transfection

pGL3 wild-type luciferase plasmid, hypoxanthine-guanine phosphoribosyltransferase (HRPT) negative control, Renilla luciferase plasmid and K529N MUT plasmid were used. A total of 1×10^6 siRNA knockdown and scrambled control cells were harvested and transfected using via electroporation using Neon™ Transfection System (MPK1096, Invitrogen) with following parameters: 1100 V, 20 ms and 2× pulses. A total of 5 μg of Firefly reporter plasmid and 0.1 μg of Renilla luciferase plasmid was used. Transfected cells were plated in a 96 well plate (5×10^4 cells/well in 100 μl) and were allowed to grow for 24 h. To analyze the transfected cells, a Dual-Luciferase assay kit (E2920 Promega) was used. One volume (100 μl) of LAR-II agent was added in each well and incubated for 15 min at room temperature with gentle shaking. After measuring the luminescence, the plate was reincubated with 100 μl STOP & GLO solution for 15 min, stopping the firefly luciferase activity and starting the Renilla luciferase activity, the luminescence was measured again. The ratio of Firefly to Renilla was calculated and used as an indicator for translational fidelity.

Statistical analysis

Statistical analysis was performed using GraphPad Prism (GraphPad 6 software). Each experiment was performed independently at least three times and for each individual experiment at least three technical replicates were used. Data is shown as mean ± standard deviation (SD). Statistical significance was calculated using unpaired two-tailed Student's t-test in GraphPad Prism software. Stars (*) in the figures represent P-values ($^*P < 0.05$, $^{**}P < 0.01$, $^{***}P < 0.001$).

Data availability

Mass spectrometry data was deposited (ProteomeXchange/MassIVE; MSV000089444, password MSV000089444_reviewer).

Supplementary Material

Supplementary Material is available at *HMG* online.

Acknowledgements

We thank Alan Lehmann for sending the transformed TTD2GL cell line. The TTDA and reconstituted controls were a kind gift of Ambra Giglia-Mari. Thomas Gronemeyer and Nils Johnson

helped with biochemical knowledge and provided access to an ultracentrifuge. Lisa Wiesmueller supported us with a fresh idea. Adrian Schelling helped with technical assistance and Meinhard Wlaschek with stimulating criticism and fruitful discussions.

Conflict of Interest statement. None declared.

Funding

German Research Foundation (DFG) by the CEMMA program (GRK1789) and the grant DFG IB83/3-4.

Author Contributions

Conceptualization, S.I.; Methodology, M.P.; Investigation, F.K., T.P., M.Q., P.M., T.L., M.A. and S.W., Resources, D.O.; Writing-Original Draft, S.I.; Writing-Review &Editing S.I., P.M., D.O., M.P. and K.S-K.; Supervision, S.I. and K.S-K. Funding Acquisition, S.I. and K.S-K.

References

1. Stefanini, M., Botta, E., Lanzafame, M. and Orioli, D. (2010) Trichothiodystrophy: from basic mechanisms to clinical implications. *DNA Repair (Amst)*, **9**, 2–10.
2. Laugel, V. (1993) Cockayne Syndrome. In Adam, M.P., Ardinger, H.H., Pagon, R.A., Wallace, S.E., Bean, L.J.H., Mirzaa, G. and Amemiya, A. (eds), *GeneReviews(R)*, Seattle (WA), in press. pmid 20301516.
3. Garinis, G.A., van der Horst, G.T., Vijg, J. and Hoeijmakers, J.H. (2008) DNA damage and ageing: new-age ideas for an age-old problem. *Nat. Cell Biol.*, **10**, 1241–1247.
4. Kuschal, C., Botta, E., Orioli, D., Digiovanna, J.J., Seneca, S., Keymolen, K., Tamura, D., Heller, E., Khan, S.G., Caligiuri, G. *et al.* (2016) GTF2E2 mutations destabilize the general transcription factor complex TFIIE in individuals with DNA repair-proficient trichothiodystrophy. *Am. J. Hum. Genet.*, **98**, 627–642.
5. Theil, A.F., Botta, E., Raams, A., Smith, D.E.C., Mendes, M.I., Caligiuri, G., Giachetti, S., Bione, S., Carriero, R., Liberi, G. *et al.* (2019) Bi-allelic TARS mutations are associated with brittle hair phenotype. *Am. J. Hum. Genet.*, **105**, 434–440.
6. Brooks, P.J. (2013) Blinded by the UV light: how the focus on transcription-coupled NER has distracted from understanding the mechanisms of Cockayne syndrome neurologic disease. *DNA Repair (Amst)*, **12**, 656–671.
7. Arseni, L., Lanzafame, M., Compe, E., Fortugno, P., Afonso-Barroso, A., Peverali, F.A., Lehmann, A.R., Zambruno, G., Egly, J.M., Stefanini, M. *et al.* (2015) TFIIH-dependent MMP-1 overexpression in trichothiodystrophy leads to extracellular matrix alterations in patient skin. *Proc. Natl. Acad. Sci. USA*, **112**, 1499–1504.
8. Traboulsi, H., Davoli, S., Catez, P., Egly, J.M. and Compe, E. (2014) Dynamic partnership between TFIIH, PGC-1alpha and SIRT1 is impaired in trichothiodystrophy. *PLoS Genet.*, **10**, e1004732.
9. Singh, A., Compe, E., Le May, N. and Egly, J.M. (2015) TFIIH subunit alterations causing xeroderma pigmentosum and trichothiodystrophy specifically disturb several steps during transcription. *Am. J. Hum. Genet.*, **96**, 194–207.
10. Compe, E., Genes, C.M., Braun, C., Coin, F. and Egly, J.M. (2019) TFIIE orchestrates the recruitment of the TFIIH kinase module at promoter before release during transcription. *Nat. Commun.*, **10**, 2084.
11. Lombardi, A., Arseni, L., Carriero, R., Compe, E., Botta, E., Ferri, D., Ugge, M., Biamonti, G., Peverali, F.A., Bione, S. *et al.* (2021) Reduced levels of prostaglandin I2 synthase: a distinctive feature of the cancer-free trichothiodystrophy. *Proc. Natl. Acad. Sci. USA*, **118**:e2024502118.
12. Iben, S., Tschochner, H., Bier, M., Hoogstraten, D., Hozak, P., Egly, J.M. and Grummt, I. (2002) TFIIH plays an essential role in RNA polymerase I transcription. *Cell*, **109**, 297–306.
13. Assfalg, R., Lebedev, A., Gonzalez, O.G., Schelling, A., Koch, S. and Iben, S. (2012) TFIIH is an elongation factor of RNA polymerase I. *Nucl. Acids Res.*, **40**, 650–659.
14. Nonnekens, J., Perez-Fernandez, J., Theil, A.F., Gadal, O., Bonnart, C. and Giglia-Mari, G. (2013) Mutations in TFIIH causing trichothiodystrophy are responsible for defects in ribosomal RNA production and processing. *Hum. Mol. Genet.*, **22**, 2881–2893.
15. Warner, J.R. (1999) The economics of ribosome biosynthesis in yeast. *Trends Biochem. Sci.*, **24**, 437–440.
16. Bradsher, J., Auriol, J., Proietti de Santis, L., Iben, S., Vonesch, J.L., Grummt, I. and Egly, J.M. (2002) CSB is a component of RNA pol I transcription. *Mol. Cell*, **10**, 819–829.
17. Lebedev, A., Scharffetter-Kochanek, K. and Iben, S. (2008) Truncated Cockayne syndrome B protein represses elongation by RNA polymerase I. *J. Mol. Biol.*, **382**, 266–274.
18. Koch, S., Garcia Gonzalez, O., Assfalg, R., Schelling, A., Schafer, P., Scharffetter-Kochanek, K. and Iben, S. (2014) Cockayne syndrome protein A is a transcription factor of RNA polymerase I and stimulates ribosomal biogenesis and growth. *Cell Cycle*, **13**, 2029–2037.
19. Okur, M.N., Lee, J.H., Osmani, W., Kimura, R., Demarest, T.G., Croteau, D.L. and Bohr, V.A. (2020) Cockayne syndrome group A and B proteins function in rRNA transcription through nucleolin regulation. *Nucl. Acids Res.*, **48**, 2473–2485.
20. Lanzafame, M., Branca, G., Landi, C., Qiang, M., Vaz, B., Nardo, T., Ferri, D., Mura, M., Iben, S., Stefanini, M. *et al.* (2021) Cockayne syndrome group A and ferrochelatase finely tune ribosomal gene transcription and its response to UV irradiation. *Nucl. Acids Res.*, **49**, 10911–10930.
21. Phan, T., Maity, P., Ludwig, C., Streit, L., Michaelis, J., Tsesmelis, M., Scharffetter-Kochanek, K. and Iben, S. (2021) Nucleolar TFIIE plays a role in ribosomal biogenesis and performance. *Nucl. Acids Res.*, **49**, 11197–11210.
22. Alupei, M.C., Maity, P., Esser, P.R., Krikki, I., Tuorto, F., Parlato, R., Penzo, M., Schelling, A., Laugel, V., Montanaro, L. *et al.* (2018) Loss of proteostasis is a pathomechanism in cockayne syndrome. *Cell Rep.*, **23**, 1612–1619.
23. Qiang, M., Khalid, F., Phan, T., Ludwig, C., Scharffetter-Kochanek, K. and Iben, S. (2021) Cockayne syndrome-associated CSA and CSB mutations impair ribosome biogenesis, ribosomal protein stability, and global protein folding. *Cells*, **10**:1616.
24. Lopez-Otin, C., Blasco, M.A., Partridge, L., Serrano, M. and Kroemer, G. (2013) The hallmarks of aging. *Cell*, **153**, 1194–1217.
25. Botta, E., Theil, A.F., Raams, A., Caligiuri, G., Giachetti, S., Bione, S., Accadia, M., Lombardi, A., Smith, D.E.C., Mendes, M.I. *et al.* (2021) Protein instability associated with AARS1 and MARS1 mutations causes trichothiodystrophy. *Hum. Mol. Genet.*, **30**, 1711–1720.
26. Botta, E., Nardo, T., Lehmann, A.R., Egly, J.M., Pedrini, A.M. and Stefanini, M. (2002) Reduced level of the repair/transcription factor TFIIH in trichothiodystrophy. *Hum. Mol. Genet.*, **11**, 2919–2928.
27. Giglia-Mari, G., Coin, F., Ranish, J.A., Hoogstraten, D., Theil, A., Wijgers, N., Jaspers, N.G., Raams, A., Argentini, M., van der Spek, P.J. *et al.* (2004) A new, tenth subunit of TFIIH is responsible for the DNA repair syndrome trichothiodystrophy group A. *Nat. Genet.*, **36**, 714–719.

28. Treaster, S.B., Ridgway, I.D., Richardson, C.A., Gaspar, M.B., Chaudhuri, A.R. and Austad, S.N. (2014) Superior proteome stability in the longest lived animal. *Age (Dordr.)*, **36**, 9597.
29. Phan, T., Khalid, F. and Iben, S. (2019) Nucleolar and ribosomal dysfunction-A common pathomechanism in childhood progerias? *Cells*, **8**:534.
30. Ke, Z., Mallik, P., Johnson, A.B., Luna, F., Nevo, E., Zhang, Z.D., Gladyshev, V.N., Seluanov, A. and Gorbunova, V. (2017) Translation fidelity coevolves with longevity. *Aging Cell*, **16**, 988–993.
31. Azpurua, J., Ke, Z., Chen, I.X., Zhang, Q., Ermolenko, D.N., Zhang, Z.D., Gorbunova, V. and Seluanov, A. (2013) Naked mole-rat has increased translational fidelity compared with the mouse, as well as a unique 28S ribosomal RNA cleavage. *Proc. Natl. Acad. Sci. USA*, **110**, 17350–17355.
32. Penzo, M., Carnicelli, D., Montanaro, L. and Brigotti, M. (2016) A reconstituted cell-free assay for the evaluation of the intrinsic activity of purified human ribosomes. *Nat. Protoc.*, **11**, 1309–1325.
33. Scharffetter-Kochanek, K., Brenneisen, P., Wenk, J., Herrmann, G., Ma, W., Kuhr, L., Meewes, C. and Wlaschek, M. (2000) Photoaging of the skin from phenotype to mechanisms. *Exp. Gerontol.*, **35**, 307–316.
34. Lerner, L.K., Moreno, N.C., Rocha, C.R.R., Munford, V., Santos, V., Soltys, D.T., Garcia, C.C.M., Sarasin, A. and Menck, C.F.M. (2019) XPD/ERCC2 mutations interfere in cellular responses to oxidative stress. *Mutagenesis*, **34**, 341–354.
35. Hayashi, M. (2009) Oxidative stress in developmental brain disorders. *Neuropathology*, **29**, 1–8.
36. Lee, J.W., Beebe, K., Nangle, L.A., Jang, J., Longo-Guess, C.M., Cook, S.A., Davisson, M.T., Sundberg, J.P., Schimmel, P. and Ackerman, S.L. (2006) Editing-defective tRNA synthetase causes protein misfolding and neurodegeneration. *Nature*, **443**, 50–55.
37. Spivak, G. and Hanawalt, P.C. (2006) Host cell reactivation of plasmids containing oxidative DNA lesions is defective in Cockayne syndrome but normal in UV-sensitive syndrome fibroblasts. *DNA Repair (Amst)*, **5**, 13–22.
38. Pascucci, B., Lemma, T., Iorio, E., Giovannini, S., Vaz, B., Iavarone, I., Calcagnile, A., Narciso, L., Degan, P., Podo, F. *et al.* (2012) An altered redox balance mediates the hypersensitivity of Cockayne syndrome primary fibroblasts to oxidative stress. *Aging Cell*, **11**, 520–529.
39. Melis, J.P., van Steeg, H. and Luijten, M. (2013) Oxidative DNA damage and nucleotide excision repair. *Antioxid. Redox Signal.*, **18**, 2409–2419.
40. Tanaka, M. and Chock, P.B. (2021) Oxidative modifications of RNA and its potential roles in biosystem. *Front. Mol. Biosci.*, **8**, 685331.
41. Argueti-Ostrovsky, S., Alfahel, L., Kahn, J. and Israelson, A. (2021) All roads lead to Rome: different molecular players converge to common toxic pathways in neurodegeneration. *Cell*, **10**, 2438.
42. Tombline, G., Gigas, J., Macoretta, N., Zacher, M., Emmrich, S., Zhao, Y., Seluanov, A. and Gorbunova, V. (2020) Proteomics of long-lived mammals. *Proteomics*, **20**, e1800416.
43. Martinez-Miguel, V.E., Lujan, C., Espie-Caullet, T., Martinez-Martinez, D., Moore, S., Backes, C., Gonzalez, S., Galimov, E.R., Brown, A.E.X., Halic, M. *et al.* (2021) Increased fidelity of protein synthesis extends lifespan. *Cell Metab.*, **33**, 2288–2300 e2212.
44. Shcherbakov, D., Nigri, M., Akbergenov, R., Brilkova, M., Mantovani, M., Petit, P.I., Grimm, A., Karol, A.A., Teo, Y., Sanchon, A.C. *et al.* (2022) Premature aging in mice with error-prone protein synthesis. *Sci. Adv.*, **8**, eabl9051.
45. Bretones, G., Alvarez, M.G., Arango, J.R., Rodriguez, D., Nadeu, F., Prado, M.A., Valdes-Mas, R., Puente, D.A., Paulo, J.A., Delgado, J. *et al.* (2018) Altered patterns of global protein synthesis and translational fidelity in RPS15-mutated chronic lymphocytic leukemia. *Blood*, **132**, 2375–2388.
46. Penzo, M., Rocchi, L., Brugiere, S., Carnicelli, D., Onofrillo, C., Coute, Y., Brigotti, M. and Montanaro, L. (2015) Human ribosomes from cells with reduced dyskerin levels are intrinsically altered in translation. *FASEB J.*, **29**, 3472–3482.
47. Lezzerini, M., Penzo, M., O'Donohue, M.F., Dos Santos, M., Vieira, C., Saby, M., Elfrink, H.L., Diets, I.J., Hesse, A.M., Coute, Y., Gastou, M. *et al.* (2020) Ribosomal protein gene RPL9 variants can differentially impair ribosome function and cellular metabolism. *Nucl. Acids Res.*, **48**, 770–787.
48. Calverley, P., Rogliani, P. and Papi, A. (2021) Safety of N-Acetylcysteine at high doses in chronic respiratory diseases: a review. *Drug Saf.*, **44**, 273–290.
49. Salas-Marco, J. and Bedwell, D.M. (2005) Discrimination between defects in elongation fidelity and termination efficiency provides mechanistic insights into translational readthrough. *J. Mol. Biol.*, **348**, 801–815.